Hammerheads Derived from sTRSV Show Enhanced Cleavage and Ligation Rate Constants†

Jennifer A. Nelson, Irina Shepotinovskaya, and Olke C. Uhlenbeck*

Department of Biochemistry, Molecular Biology and Cell Biology, Northwestern University, 2205 Tech Drive, Hogan 2-100, Evanston, Illinois 60208

Received June 13, 2005; Revised Manuscript Received August 31, 2005

ABSTRACT: The catalytic properties of the hammerhead ribozyme embedded in the (+) strand of the satellite tobacco ringspot viral genome are analyzed with the goal of obtaining the elemental rate constants of the cleavage (k_2) and ligation (k_{-2}) steps. Two different chimeras combining the sTRSV (+) hammerhead and the well-characterized hammerhead 16 were used to measure the cleavage rate constant (k_2), the rate of approach to equilibrium ($k_{obs} = k_2 + k_{-2}$), and the fraction of full-length hammerhead at equilibrium ($k_{-2}/k_2 + k_{-2}$). When compared to minimal hammerheads that lack the recently discovered loop I−loop II interaction, an extended format hammerhead derived from sTRSV studied here shows at least a 20-fold faster k_2 and a 1300-fold faster k_{-2} at 10 mM $MgCl_2$. However, the magnesium dependence of the cleavage rate is not significantly changed. Thus, the enhanced cleavage of this hammerhead observed in vivo is due to its higher intrinsic rate and not due to its tighter binding of magnesium ions. The faster k_{-2} of this hammerhead suggests that ligation may be used to form circular RNA genomes. This in vitro system will be valuable for experiments directed at understanding the hammerhead mechanism and the role of the loop I−loop II interaction.

The hammerhead ribozyme is an RNA self-cleavage motif present in the genomes of plant viroids and satellite RNAs of plant viruses (*1*−*4*). Minimal hammerheads were initially defined as having three nonconserved helices intersecting at a conserved catalytic core of 15 nucleotides (*5*−*7*). Recently, it has been shown that many, if not all, hammerheads present in natural RNAs have additional, nonconserved, structural elements that are essential for cleavage in vivo (*8*, *9*) or in vitro (*10*). In many cases, such as in the satellite RNA of tobacco ringspot virus (sTRSV), this added element is a specific tertiary interaction between hairpin loops at the ends of helix I and helix II, which are spatially close in the X-ray crystal structures of minimal hammerheads (*11*, *12*). In other cases, such as with the hammerhead from *Schistosoma mansoni*, a tertiary interaction between a hairpin loop at the end of helix II and an internal loop in helix I is required for rapid cleavage (*13*, *14*). In vitro cleavage of these extended hammerheads indicates that the tertiary interaction permits more rapid cleavage than minimal hammerheads at the lower magnesium ion concentrations present within cells (*8*, *9*, *13*, *14*). Recent FRET experiments show that *Schistosoma* hammerhead also folds at lower magnesium ion concentrations, suggesting that these hammerheads bind magnesium ions more tightly (*15*). However, rapid reaction kinetics of *Schistosoma* hammerhead indicated that, although it cleaves much faster than minimal hammerheads, very high concentrations of magnesium ions are required to reach the maximum rate of cleavage (*14*).

Viroid genomes which possess hammerhead sequences are often present as both linear and circular RNAs (*2*, *16*, *17*), and the plus strand of sTRSV exists as an equimolar mixture of linear and circular RNA in vivo (*18*, *19*). It has been postulated that circular genomes arise from hammerhead-catalyzed ligation of linear genomes (*3*, *16*). However, when measured with minimal hammerheads, the reverse reaction is approximately 100- fold slower than the cleavage reaction, yielding less than 1% of ligated hammerheads at equilibrium (*20*). Thus, it is of interest to determine whether the greater proportion of circular genomes inside cells could partially be the result of a faster rate of ligation for the extended hammerheads that are embedded in their genomes. In all of the kinetic experiments on extended hammerheads reported thus far, apparent rates of cleavage are measured, and it is often unclear whether the reverse, ligation reaction is occurring at the same time. If ligation does occur, then the apparent cleavage rate, k_{obs}, equals the sum of the cleavage rate constant, k_2, and the ligation rate constant, k_{-2}. If ligation does not occur, $k_{obs} = k_2$. In either case, the value of k_{-2} remains unknown. The goal of this work is to establish a kinetically well characterized extended hammerhead that permits measurement of both of the rate constants. This system can then be used to evaluate the effects of varying magnesium ion concentration, pH, and temperature on cleavage and ligation separately.

MATERIALS AND METHODS

RNA Oligonucleotides. Synthetic DNA oligonucleotides were used to clone the catalytic portion of HH16-T1 and the full-length HH16-T2 behind the T7 promoter into

† This work was supported by NIH Grant GM036944-21.

* To whom correspondence should be addressed. Telephone: 847-491-5139. Fax: 847-491-5444. E-mail: o-uhlenbeck@northwestern.edu.

10.1021/bi051130t CCC: $30.25
Published on Web 10/14/2005

pUC18. After linearizing the plasmid with *Sma*I, in vitro transcription using T7 RNA polymerase (*21*) and purification on denaturing polyacrylamide gels yielded the 46-nucleotide HH16-T1 and the cleaved 49-nucleotide HH16-T2 ribozymes. HH16-T1M was transcribed directly from primer-extended synthetic DNA. The uncleaved 58-nucleotide HH16-T2 was synthesized in a T7 transcription reaction containing a 20 μM amount of a 25-nucleotide inhibitory oligonucleotide (5′CGGACTCATCAGACCGGACACAT 3′) with [α-^{32}P]ATP (3000 Ci/mmol), quenched in a stop mix containing 30 mM EDTA,[1] purified on 8% polyacrylamide gels and eluted in 5 mM EDTA to prevent self-cleavage (*8*, *9*), ethanol precipitated, and stored in water at −20 °C. The 12mer substrate strand, P1-GUC, for the HH16-T1 reaction was made by chemical synthesis (Dharmacon Research, Boulder, CO), purified using 20% denaturing polyacrylamide gel electrophoresis (*22*), and 5′ end labeled using [γ-^{32}P]ATP (approximately 6000 Ci/mmol) and T4 polynucleotide kinase. [5′-^{32}P]P1-GUC was purified on a MicroSpin G-25 (Amersham Biosciences) spin column to remove excess [γ-^{32}P]-ATP and exchange the buffer into water. [5′-^{32}P]P1 was prepared from [5′-^{32}P]P1-GUC by incubating with 5 μM HH16 ribozyme in 50 mM Hepes, pH 7.5, and 10 mM $MgCl_2$ in a 25/40 °C thermocycle (5−8 intervals) to maximize the extent of cleavage. In some cases, <10% labeled P1-GUC remained present in the [5′-^{32}P]P1 preparations, but control experiments with HH16-T2 ribozyme showed that the remaining [5′-^{32}P]P1-GUC was not cleaved in lengthy incubations.

Rate Measurements. Bimolecular cleavage or ligation assays were carried out essentially as described previously (*20*, *23*). Ribozyme (2 μM) (HH16-T1, HH16-T1M, or HH16-T2) was incubated with trace (<2 nM) 5′-^{32}P-labeled substrate (P1-GUC for the cleavage assay or P1 for the ligation assay) in 50 mM Mes, pH 6.0, for 2 min at 95 °C, allowed to slow cool to 40 °C over 30 min, and then incubated at room temperature for 10 min. Aliquots of 20 μL were then placed in a 96-well plate, and the reactions were initiated with the addition of 20 μL of 50 mM Mes, pH 6.0, and double the desired final $MgCl_2$ concentration. A ribozyme titration assay confirmed that all of the substrate was bound under these conditions. Additionally, chemically synthesized HH16-T1 and HH16-T1 transcribed in the presence of GMP were also tested. At 50 mM Mes, pH 6.0, and 10 mM Mg^{2+} these variations had no effect on the measured rate constant. Methanol was used as a cryoprotectant for certain low-temperature incubations (*24*). For reactions carried out at pH 7.0 and 7.5, Hepes buffer was used instead of Mes. Time points (3 μL) were quenched in 15 μL of stop solution (7 M urea, 50 mM EDTA, and 0.02% bromophenol blue and xylene cyanol dyes) on ice and the products fractionated on 20% denaturing PAGE. The bands were imaged with a Molecular Dynamics Storm Phosphoimager (Amersham Biosciences) and quantified using ImageQuant (Amersham Biosciences). The data were fit as described previously (*25*). Independent experiments show variations in rates of no greater than 2-fold.

[1] Abbreviations: MES, 2-(*N*-morpholino)ethanesulfonic acid; Tris-HCl, tris(hydroxymethyl)aminomethane hydrochloride; EDTA, ethylenediaminetetracetic acid; Hepes, *N*-(2-hydroxyethyl)piperazine-*N*′-2-ethanesulfonic acid; SDS, sodium dodecyl sulfate.

Unimolecular self-cleavage of HH16-T2 was performed essentially as described by Khvorova et al. (*8*). Full-length ribozyme (final concentrations 0.1−0.3 μM) was heated in 50 mM Mes, pH 6.0, to 95 °C for 2 min, slow cooled for 30 min, and incubated at 25 °C for 10 min. At this stage, despite all precautions, up to 30% of the hammerhead was already cleaved. Since P1 is unlikely to remain associated during purification, these cleaved hammerheads were presumed not to be active. Cleavage was initiated by the addition of Mg^{2+}, and the rate and extent of cleavage were calculated from the change in the fraction of full-length hammerhead that occurred.

Cleavage reactions in the presence of LiCl were carried out as described previously (*26*, *27*). Reaction mixtures containing 50 mM Hepes (pH 7.5), 1 μM ribozyme (HH16-T1 or HH16-T2), trace-labeled substrate (P1-GUC or P1), and 0.9 mM EDTA were heated to 95 °C for 2 min, allowed to cool, and incubated at 25 °C for 10 min. The reactions were then aliquoted into 96-well plates and initiated by the addition of the desired LiCl concentrations. Similar experiments have shown rate variations up to 3-fold. LiCl was 99.99+ pure from Aldrich.

Coupled transcription cleavage reactions were performed as described by Long and Uhlenbeck (*28*). A 50 μL transcription reaction contained 50 μg of T7 RNA polymerase, 4 mM each NTP, and 20 μCi of [α-^{32}P]ATP, 40 mM Tris-HCl buffer, pH 8.1, and 17 mM $MgCl_2$. The reaction was initiated by the addition of 5 μL of 1 μg/μL plasmid DNA template, and 5 μL aliquots were removed at the indicated times, quenched in 9 μL of stop solution, and analyzed on 10% denaturing polyacrylamide gels.

To measure the fraction of full-length hammerhead at equilibrium, the cleaved 49-nucleotide HH16-T2 was mixed with trace [5-^{32}P]ATP-labeled P1 in 50 mM Mes, pH 6.0, at 95 °C for 2 min, slow cooled to 40 °C over 30 min, and then incubated at room temperature for 10 min. The reactions were initiated with the addition of $MgCl_2$ to the desired concentrations and incubated for 45 min to reach equilibrium (4 h for $MgCl_2$ concentrations ≤0.1 mM). Aliquots of 2 μL were quenched in 10 μL of stop solution (see above) on ice and were loaded on 20% denaturing polyacrylamide gels. After quantitation, the data were fit to a simple binding equation $f_{lig} = (f_{ligmax}[Mg])/(K_{app}(Mg) + [Mg])$, where f_{lig} = the fraction ligated at a given magnesium concentration and f_{ligmax} = the fraction ligated at infinite magnesium concentration. The percent ligated varied for a given set of conditions by up to 2-fold.

RESULTS

The hammerhead embedded in the (+) strand of sTRSV RNA (Figure 1A) was shown by Khvorova et al. (*8*) to contain the loop I−loop II interaction that leads to effective cleavage in vivo. However, the length of helix III in this hammerhead is too short to permit stable association of P1, the 5′ reaction product, thereby prohibiting the reverse, ligation reaction to be measured (*25*). This prompted the design of two new hammerheads that contain the loop I−loop II elements of sTRSV hammerhead but are primarily hammerhead 16 (Figure 1B), a bimolecular hammerhead which has a longer helix III and has been extensively characterized biochemically (*20*, *29*, *30*). By containing a

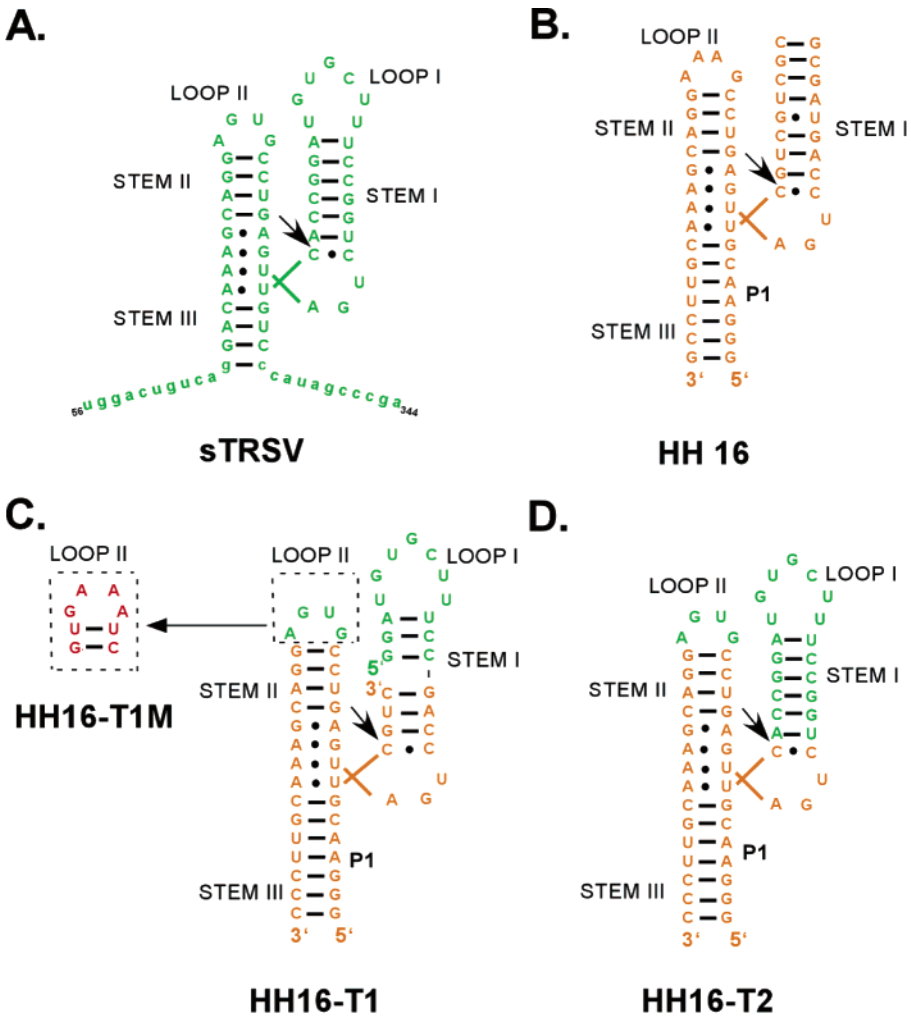

FIGURE 1: Hammerhead secondary structures depicted in a manner that reflects the X-ray structure with the cleavage site indicated by the arrow. Stems and loops are defined by structural nomenclature (*50*). (A) The natural hammerhead contained in the satellite RNA of tobacco ringspot virus is shown in capital letters, and the immediate flanking sequences are shown in lower case. (B) Hammerhead 16, a well-characterized minimal hammerhead (*20*). (C) The bimolecular HH16-T1 containing the sTRSV sequences in green and the HH16 sequence in orange. A nick in the phosphate backbone between 1.3 and 1.4 is present in stem I. A difference in loop II defines HH16-T1M (red). (D) The unimolecular HH16-T2 containing the sTRSV sequence in green and HH16 sequences in orange. Both HH16-T1 and HH16-T2 have the same 5′ cleavage product, P1, as HH16.

high proportion of the hammerhead 16 sequence, the new hammerheads are less likely to form the alternate folded conformers that can lead to incomplete cleavage or other kinetic heterogeneities (*13*, *25*, *31*). The first new hammerhead, termed HH16-T1 (Figure 1C), consists of two annealed oligonucleotides, a 46-nucleotide ribozyme and a 12-nucleotide substrate. The substrate sequence is identical to P1-GUC, a fully active substrate of hammerhead 16, and cleaves to give a nine nucleotide 5′ product and a three nucleotide 3′ product. After cleavage the longer 5′ product P1 will be bound to the ribozyme through eight base pairs, and measurements with HH16 indicate that it dissociates at 0.04 min^{-1} at 25 °C, much longer than the time scale of a typical experiment (*20*). In contrast, the 3′ product uses only three base pairs to bind to the ribozyme and therefore dissociates very rapidly (<1 s^{-1}), so the reverse, ligation reaction cannot occur (*20*, *23*, *25*, *32*). The second hammerhead, termed HH16-T2 (Figure 1D), is a single 58-nucleotide RNA molecule which is expected to cleave and give the same nine nucleotide 5′ product, P1, and a 49-nucleotide 3′ product corresponding to the rest of the hammerhead. In this case, the slow dissociation of the 5′ product will allow the reverse, ligation reaction to occur (*20*). Thus, like hammerhead 16, HH16-T2 will be a mixture of cleaved and ligated forms at equilibrium.

Direct Measurement of k_2 Using the Cleavage of HH16-T1. Cleavage of HH16-T1 is performed as a bimolecular reaction using a saturating concentration of ribozyme (1 μM) and trace ^{32}P substrate in 50 mM Mes at pH 6.0 at 10 mM $MgCl_2$ at room temperature. The low pH was used to permit the cleavage rate to be measured using manual pipetting. Under these conditions, the rate of binding of substrate is fast compared to the rate of cleavage (*20*) and fits a single exponential, consistent with a single active species. The extent of cleavage is greater than 70%, indicating that the majority of molecules are in the active conformation. Under the reaction conditions, HH16-T1 has an observed cleavage rate, $k_{obs} = 0.62 \pm 0.13$ min^{-1} (Table 1). Since ligation does not occur, $k_{obs} = k_2$, the cleavage rate constant. This value is approximately 20 times faster than the $k_2 = 0.03$ min^{-1} of HH-16 corrected to pH 6.0 (*20*, *30*). A mutant hammerhead, HH16-T1M (Figure 1C), where the loop I−loop II interaction is disrupted by replacing the native sTRSV loop II sequence with loop II of PLMVd hammerhead, shows k_2

Table 1: Average Rate Constants of Hammerhead Cleavage and Ligation at pH 6.0

	10 mM $MgCl_2$		1 mM $MgCl_2$	
	k_2 (min^{-1})	k_{-2} (min^{-1})	k_2 (min^{-1})	k_{-2} (min^{-1})
HH16-T1	0.62		0.15	
HH16-T2	1.67	0.23	0.53	0.034
HH16	0.03[a,b]	2.5×10^{-4} [a]	0.004[b,c]	

[a] Value from ref *20* corrected for pH. [b] Value from ref *30* corrected for pH. [c] *V*alue from ref *49* corrected for pH.

$= 0.040 \pm 0.006\ min^{-1}$ (Figure 2A), which is 15-fold slower than HH16-T1 but about 1.5-fold faster than HH16 under the same conditions. While it is possible that the mutation in HH16-T1M does not fully disrupt the loop I−loop II interaction, it is clear that the loops contribute substantially to the rate of cleavage.

The reactivity of HH16-T1 was measured over a range of pH values between 4.7 and 7.5 in buffer containing 50 mM Mes for the lower values and 50 mM Hepes for values of 7.0 and above (data not shown). In the narrow range of pH 5.5−6.5 HH16-T1 was found to have a similar log-linear relationship between pH and rate as reported for other hammerheads, both minimal and extended (*14*, *29*, *33*). At pH 5.0 and below the reaction rate is less than expected, presumably because the RNA structure is unstable as a result of protonated bases. Conversely, at pH values greater than 6.5, HH16-T1 is too fast to measure accurately using manual methods. However, since proton transfer rates are fast, it is assumed that the log-linear relationship between rate and pH can be extrapolated to higher pH values, permitting comparison with data of minimal hammerheads usually collected at pH 7.5.

In addition to pH, temperature has been shown to affect cleavage rates of minimal hammerheads (*24*, *29*). Examination of the cleavage rate of HH16-T1 as a function of temperature revealed that, like with the minimal hammerheads, the rate of cleavage increases with increasing temperature (Figure 2B). When the data are reported on an Arrhenius plot, the temperature dependence of the rate shows a linear relationship between 5 and 37 °C, having an $E_a =$ 7.3 kcal/mol. At temperatures greater than 37 °C, the cleavage rate for HH16-T1 no longer increases, unlike what is seen for other cis extended hammerheads which show a linear Arrhenius plot up to 55 °C (*34*). The leveling off seen for HH16-T1 is most likely due to the fact that the short, three base helix that is part of stem I begins to "fray", preventing formation of the active structure at higher temperatures, a phenomenon known to occur with other hammerheads (*23*, *35*).

The rate of hammerhead cleavage is known to be affected by magnesium ion concentration (*30*, *36*, *37*). HH16-T1 and HH16-T1M cleavage rates were measured at magnesium ion concentrations ranging from 500 μM to 400 mM at pH 6.0. Under these conditions, data can be collected using manual pipetting techniques and compared to other hammerheads. As shown in Figure 2C, the log of the cleavage rate for both hammerheads increases linearly with the log of magnesium ion concentration at every ion concentration tested. The slope of the plots are both less than unity ($m = 0.48$ and 0.55), indicating that cooperative binding of the Mg^{2+} ion does not occur. This behavior is similar to that of several minimal

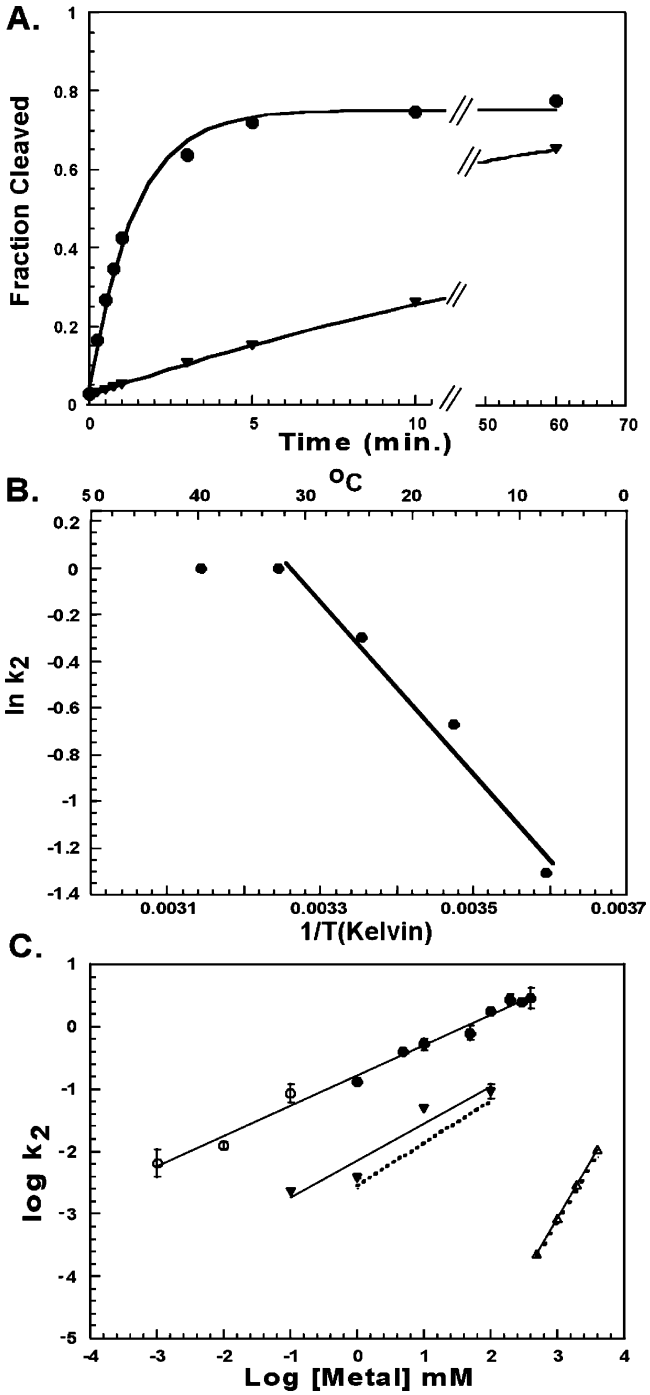

FIGURE 2: Cleavage properties of HH16-T1 and HH16-T1M. (A) Single turnover cleavage at saturating ribozyme and trace substrate concentrations for HH16-T1 (○) and HH16-T1M (▼) in 50 mM Mes, pH 6.0, and 10 mM Mg^{2+} at 25 °C. $k_2 = 0.62 \pm 0.13\ min^{-1}$ for HH16-T1 and 0.040 ± 0.006 min for HH16-T1M. Nearly 70% completion for HH16-TIM was reached by 60 min, indicating that the slower rate is not the result of a greater population of misfolded molecules. (B) Arrhenius plot for HH16-T1 in 1 mM $MgCl_2$. $E_a =$ 7.3 kcal/mol for the linear part of the curve. (C) Metal ion concentration dependence of the cleavage rate for various hammerheads at pH 6. HH16-T1 magnesium ion data were taken at pH 6.0 (●) or pH 7.0 and divided by 10 (○) with slope = 0.48. Magnesium ion data were for HH16-T1M (▼) with slope = 0.56. The dotted line (···) is magnesium ion data for HH16 taken from Clouet d'Orval et al. (*30*) and divided by 10 to correct to pH 6.0 with slope = 0.67. Lithium ion data for HH16-T1 (Δ) were obtained at pH 7.5 and divided by 31.6 to correct to pH 6.0 with slope = 1.7. The dashed line (- - -) is lithium ion data for the minimal HH8 (*27*) corrected in the same way.

hammerheads [HH16, $m = 0.66$ (*30*); HH8, $m = 0.7$ (*27*)]. In addition, there is no indication that the rate for HH16-T1 saturates at high magnesium ion concentration. While this has been observed (*37*), saturation at modest magnesium concentrations is more commonly observed for hammerheads (*27*, *30*, *33*, *36*, *38*−*41*). To obtain data at even lower magnesium ion concentrations, data were collected at pH 7.0. At 0.1 mM Mg^{2+}, pH 7.0, $k_2 = 0.86 \pm 0.13$ min^{-1} for HH16-T1, which agrees well with the $k_{obs} = 1.2$ min^{-1} reported by Khvorova et al. (*8*) for a slightly different sTRSV hammerhead under very similar conditions. When the pH 7.0 data are corrected to pH 6.0 (open circles in Figure 2C), it is clear that HH16-T1 continues to cleave about 20-fold faster than minimal hammerheads at magnesium ion concentrations as low as 1 μM. This suggests that the loop I−loop II interaction stimulates hammerhead cleavage equivalently well over a wide range of magnesium concentrations.

Hammerhead catalysis can also be stimulated in high concentrations of monovalent ions (*26*, *27*, *42*). The cleavage rate of HH16-T1 was determined at a series of lithium ion concentrations between 0.5 and 4 M and 50 mM Hepes, pH 7.5, in the presence of 0.4 mM EDTA to chelate any trace divalent ions present. At every lithium ion concentration tested, the observed cleavage rates were identical to those previously determined for a minimal hammerhead (*27*). When the data are corrected to pH 6.0 and plotted in Figure 2C, it is clear that cleavage of extended hammerheads in lithium ions is much slower than in magnesium ions. Taken together, the data suggest that, in the presence of lithium ions, the favorable tertiary interactions between loop I and loop II do not form or, if they do form, are unable to enhance catalysis.

Approaching Equilibrium with HH16-T2 Using both Ligation and Cleavage Reactions. The approach to equilibrium for HH16-T2 was measured using either the forward, cleavage reaction or the reverse, ligation reaction. To obtain full-length HH16-T2, the in vitro transcription reaction contained a single-stranded DNA oligonucleotide complementary to the hammerhead core that prevented cleavage (*8*, *9*). After purification, the full-length HH16-T2 was prefolded in a buffer without magnesium, and cleavage was initiated by the addition of magnesium to the desired concentration. For the ligation reaction, the [5′-^{32}P]P1 oligonucleotide was preincubated with the purified 49-nucleotide fragment corresponding to the rest of HH16-T2, and the reaction was initiated by the addition of magnesium ions to the desired concentration. Both the measured rate, $k_{obs} = k_2 + k_{-2}$, and the fraction of full-length hammerhead at equilibrium, $f_{eq} = k_{-2}/k_2 + k_{-2}$, would be expected to be the same regardless of the path taken to reach equilibrium (*20*, *25*). Figure 3A shows the approach to equilibrium from both the forward and reverse direction in 50 mM Mes, pH 6.0, and 1 mM Mg^{2+}. As expected, the observed rate of cleavage [k_{obs}(cleavage) $= 0.54 \pm 0.17$ min] is the same as the observed rate of ligation [k_{obs}(ligation) $= 0.59 \pm 0.10$ min]. However, the fraction of full-length HH16-T2 at equilibrium deduced from the cleavage reaction, f_{eq}(cleavage) $= 0.48 \pm 0.08$, was considerably more than the same value deduced from the ligation reaction, f_{eq}(ligation) $= 0.06 \pm 0.013$. The fact that the two assays do not meet at the same equilibrium point indicates that a fraction of the molecules

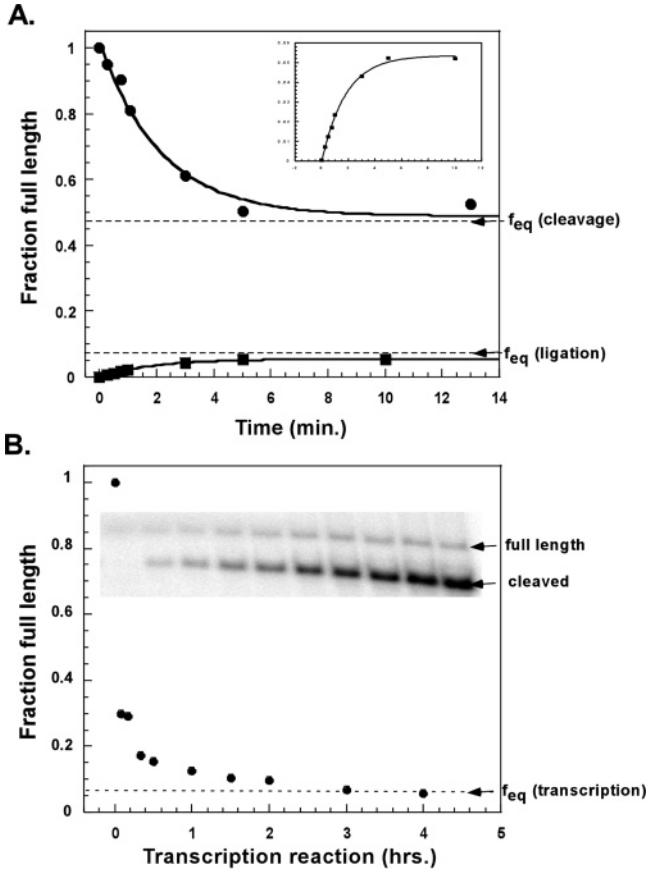

FIGURE 3: (A) Approach to equilibrium for HH16-T2 in 50 mM Mes, pH 6.0, and 1 mM $MgCl_2$. Cleavage reaction (●) with $k_{obs} = 0.54 \pm 0.17$ min^{-1} and f_{eq} (cleavage) $= 0.48 \pm 0.08$. Ligation reaction (■) with $k_{obs} = 0.59 \pm 0.10$ min^{-1} and f_{eq} (ligation) $= 0.06 \pm 0.013$ (also in inset). (B) Coupled transcription cleavage of HH16-T2. The fraction of full-length hammerhead remains constant as transcription proceeds: f_{eq}(transcription) $= 0.06 \pm 0.008$.

in one or both of the reactions were inactive, presumably because they were misfolded during renaturation after purification on denaturing gels.

To assess HH16-T2 cleavage without renaturation, cleavage was measured during in vitro transcription, as had been done for an intramolecular version of HH16 (*43*). A coupled transcription−cleavage assay was performed at 25 °C in 40 mM Tris-HCl, pH 8.1, 16 mM NTPs, and 17 mM $MgCl_2$, giving a free magnesium ion concentration of 1 mM, similar to that used in Figure 3A. As shown in Figure 3B, the fraction of full-length HH16-T2 decreases rapidly and reaches a final value of f_{eq}(transcription) $= 0.06 \pm 0.008$. Although it is possible to extract k_{obs} from such data (*43*), the cleavage and ligation rate constants of HH16-T2 are expected to be very fast at pH 8.1; therefore, the observed rate must reflect some other process. To address this, a pulse−chase experiment was performed where a nonradioactive reaction similar to Figure 3B was initiated, [α-^{32}P]ATP added after 10 min, transcription terminated 10 min later by the addition of SDS, and the fraction of full-length RNA analyzed as a function of time as before. A kinetic profile very similar to Figure 3B was observed (data not shown), indicating that the slow rate is unlikely to be due to transcriptional initiation and probably reflects a rate-limiting conformational change for at least part of the HH16-T2 molecules. To test this possibility, a pulse-labeled transcription reaction was terminated with EDTA, heated to 95 °C

for 2 min, and cooled to 25 °C. Upon addition of $MgCl_2$ to this reaction, cleavage was immediate and reached the same $f_{eq} = 0.06$ obtained in Figure 3B (data not shown). Taken together, these experiments support the view that the rate observed in Figure 3B is not the chemical cleavage rate but a slower conformational change. However, the value of f_{eq}(transcription) = 0.06 reflects the final value for the hammerhead equilibrium. This in turn implies that the cleavage reaction in Figure 3A contained 42% inactive hammerheads, whereas the ligation reaction contained nearly no inactive hammerheads. In other words, the 58-nucleotide full-length RNA was incompletely renatured after purification on denaturing gels, but the shorter 49-nucleotide ribozyme, HH16-T2, was fully renatured.

The value of $k_{obs} = k_2 + k_{-2}$ and $f_{eq} = k_{-2}/k_2 + k_{-2}$ (for HH16-T2) can be used to calculate the individual forward and reverse rate constants. Using the average value of k_{obs}(cleavage) and k_{obs}(ligation) of 0.57 min^{-1} and f_{eq}(ligation) = f_{eq}(transcription) = 0.06, values of $k_2 = 0.53$ min^{-1} and $k_{-2} = 0.034$ min^{-1} are obtained for 1 mM $MgCl_2$. Similar experiments established a $k_2 = 1.67$ min^{-1} and a $k_{-2} = 0.23$ min^{-1} at 10 mM $MgCl_2$ (Table 1). Similar to minimal hammerheads, HH16-T2 has a rate of approach to equilibrium dominated by the cleavage rate constant and, therefore, is mostly cleaved at equilibrium. However, although k_2 still dominates, k_{-2} has been increased substantially, and thus, the "internal" equilibrium for HH16-T2 is $K_{int} = k_2/k_{-2} =$ 16 at 1 mM $MgCl_2$ and 7.3 at 10 mM $MgCl_2$. These values are shifted considerably further toward ligation than HH16 ($K_{int} = 130$ at 10 mM $MgCl_2$) (*20*). Thus, it appears that one role of the tertiary interactions in the extended hammerhead, HH16-T2, is to increase the relative rate of ligation with respect to cleavage.

The more convenient and accurate ligation reaction was used to further characterize the catalytic properties of HH16-T2. The temperature dependence of the k_{obs} was measured from −20 to 25 °C. As is the case with HH16 and HH16-T1, k_{obs} for HH16-T2 decreases with decreasing temperatures (*24*). If the assumption is made that the percent total active molecules does not change with changing temperatures, Arrhenius plots for k_2 and k_{-2} of HH16-T2 using the experimental k_{obs} and f_{eq}(ligation) values can be calculated (Figure 4A). The k_{obs} for the forward reaction appears to be more affected by changing temperatures than the reverse reaction, giving E_a(cleavage) = 10.0 kcal/mol and E_a(ligation) = 2.8 kcal/mol. The value of E_a(cleavage) is similar to the $E_a = 7.3$ kcal/mol for HH16-T1. Similar behavior is seen for HH16, E_a(cleavage) = 22 kcal/mol and E_a(ligation) = 10 kcal/mol (*29*). Since the ligation rate is less affected by temperature than the cleavage rate, the fraction of full-length molecules at equilibrium increases with decreasing temperatures, reaching 20% at −20 °C.

As is the case with HH16-T1, k_{obs} for HH16-T2 increases with increasing magnesium ion with a similar slope (m = 0.44) and fails to saturate 100 mM Mg^{2+} (data not shown). The fraction of full-length molecules increases with increasing magnesium concentration and exhibits a simple binding behavior with a $K_{app}(Mg^{2+})$ of 1.6 mM (Figure 4B). HH16 shows a similar behavior but with a higher $K_{app}(Mg^{2+})$ = 13 mM (*29*). Finally, k_{obs} of HH16-T2 in 4 M LiCl at pH 7.5 is 0.47 min^{-1} (data not shown), which is similar to the value for HH16-T1 ($k_2 = 0.33$ min^{-1}) and HH8 (k_{obs} = approximately 0.32 min^{-1}), another minimal hammerhead very similar to HH16 (*27*, *44*), confirming that the tertiary interactions do not stimulate cleavage in this buffer.

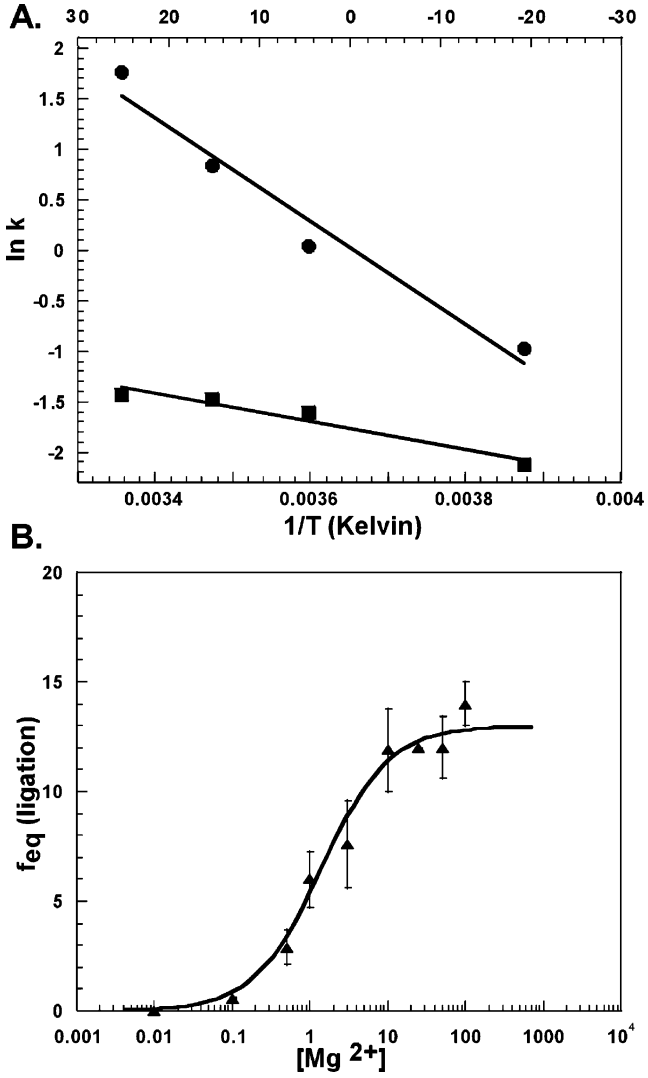

FIGURE 4: (A) Arrhenius plots for HH16-T2 in 1 mM $MgCl_2$ for k_2 (●) and k_{-2} (■) assuming a constant total percent active molecules. E_a(cleavage) = 10.0 kcal/mol. E_a(ligation) = 2.8 kcal/mol. (B) f_{eq}(ligation) of HH16-T2 as a function of magnesium ion concentration in 50 mM Mes, pH 6.0. The line corresponds to a best fit binding curve with $K_{app}(Mg^{2+}) = 1.6$ mM.

DISCUSSION

The goal of this work was to obtain values of k_2 and k_{-2}, the forward and reverse rate constants for the cleavage step of the sTRSV(+) hammerhead, which is a member of the group of hammerheads that contain a stabilizing tertiary interaction between loop I and loop II. A study of the cleavage kinetics of this group of hammerheads is complicated by the need to avoid disrupting the tertiary interaction by introducing a break in the phosphodiester backbone within loop I or loop II. Thus, the bimolecular formats usually used to study hammerhead kinetics (*25*) were not appropriate. One approach to convert the sTRSV (+) hammerhead into a bimolecular format involved changing loop II into an internal loop, but this only slightly improved cleavage compared to a minimal hammerhead, suggesting that the tertiary interaction had been disrupted (*45*). In an alternative attempt to

overcome this limitation, we introduced a break in the chain between residues 1.3 and 1.4 in the middle of stem I, thereby preserving the tertiary interaction. This approach, embodied in HH16-T1, allowed cleavage to be measured in the conventional bimolecular format but only gave k_2 and not k_{-2}. In addition, the value of k_2 for HH16-T1 was only slightly slower than that deduced from its intact counterpart, HH16-T2. The major variance between the two is the distinctly different temperature dependence of the cleavage rate which is likely due to "fraying". In addition, the presence of the nick close to the cleavage site subtly alters the dynamics of this hammerhead, marginally reducing the rate of cleavage. While it was not explored, it is possible that placing the nick at other sites in stem I would yield a form of a bimolecular sTRSV hammerhead less susceptible to fraying and, thus, more active at higher temperature.

The conventional way to obtain k_2 and k_{-2} is to follow the approach to equilibrium of a hammerhead in a unimolecular self-cleavage reaction and bimolecular ligation reaction. It is necessary to perform both reactions to test whether the same equilibrium is reached from each direction. To adapt this assay for the sTRSV hammerhead, it was necessary to lengthen stem III so that the cleaved products remain stably bound to one another. While this approach was successful in the sense that both reactions gave similar apparent cleavage rates, they did not reach the same equilibrium value, indicating that one or both reactions contained a portion of inactive molecules. Since the inactive hammerheads are presumably the result of misfolding that occurred during purification, we attempted a number of different renaturation protocols without improving the situation. As a result, the successful dissection of k_2 from k_{-2} ultimately required an independent measurement of the equilibrium point in a coupled transcription−cleavage assay which had to be done at slightly different reaction conditions. Interestingly, the value of f_{eq}(transcription) was nearly identical to that obtained in the ligation reaction, indicating that for HH16-T2 k_2 and k_{-2} can be deduced by approaching the equilibrium from the ligation side but not the cleavage side of the reaction.

A number of clear conclusions can be drawn from this analysis of the cleavage and ligation properties of the sTRSV hammerhead. First of all, in agreement with several others (*8*, *9*, *13*, *14*), it is clear that the apparent cleavage rate k_{obs} is considerably faster than corresponding minimal hammerheads. We now know this increase is due to both a faster k_2 and a faster k_{-2}. The sTRSV hammerhead shows a k_2 that is at least 20-fold faster than HH16 at 10 mM $MgCl_2$. It is clear that this increase is due to the loop−loop interactions since a mutation in loop II dramatically decreases the rate constant. However, from a mechanistic perspective it is unclear why the rate constant is so much faster. The tertiary interaction could either raise the ground state or lower the transition state of the reaction. Since Wang et al. (*46*) have proposed an additional isomerization step prior to the transition state that involves the docking of domains 1 and 2 of the catalytic core, it is tempting to propose that the tertiary interactions would shift the docking equilibrium toward the closed form, thereby lowering the energy required to achieve the active conformation. Clearly, additional mechanistic experiments will be required to address this point.

The dependence of k_2 on magnesium concentration for the sTRSV extended hammerhead does not show saturation or cooperative binding. Failure to reach saturation does not resemble most minimal hammerheads but is similar to that of the *S. mansoni* hammerhead (*13*, *14*). Since multiple magnesium ions are involved in the folding of any hammerhead, it is difficult to make any specific conclusions about the role of the magnesium ions in the cleavage mechanism. It is interesting that the HH16-T1 and HH16-T2 hammerheads do not cleave faster than a minimal hammerhead in LiCl. Whether this is due to nonproductive folding of the tertiary elements in the monovalent ion, an additional divalent binding site required by the loop I−loop II interaction, or is simply a concentration issue cannot be resolved here. However, this suggests that the loop−loop interaction, like many tertiary interactions, requires magnesium ions to form productively. In any case, since the sTRSV hammerhead does not show a significant difference from minimal hammerheads in the magnesium dependence of k_2, its improved ability to cleave in vivo, where magnesium ion concentration is low, is simply due to its faster intrinsic cleavage rate and not due to its ability to bind magnesium ions unusually tightly.

An important conclusion of this work is that k_{-2}, the reverse ligation rate constant of the sTRSV hammerhead, is elevated by even more than the forward rate constant when compared to a minimal hammerhead. The value of k_{-2} for HH16-T2 is 1300-fold faster than the corresponding value for HH16 at 10 mM $MgCl_2$. This large increase in the ligation rate was not unexpected based on properties of hammerheads with chemical cross-links between stem I and stem II (*47*, *48*). In those works it was proposed that the cross-link reduced the modes of motion available to the cleaved hammerhead, permitting a more facile attack of the 5′-hydroxyl on the 2′,3′-cyclic phosphate than when the cross-link was absent. It seems reasonable that a similar explanation can be used for the improved ligation rate of the extended hammerhead, since the tertiary interactions could also improve the positioning of the reactive groups. It is interesting that several of the chemical cross-linked hammerheads are actually much more effective at promoting ligation than the tertiary interactions in HH16-T2. For example, with one cross-linked hammerhead at 4 °C, k_{-2} actually exceeds k_2 (*47*), a situation that is not seen for sTRSV under any condition tested. However, it is important to note that the chemically cross-linked hammerheads do not affect k_2 at all. Thus, while it is clear that the tertiary interactions of the extended hammerhead increase k_{-2} by improving positioning in the cleaved hammerhead, they also contribute to the enhanced rate by altering the transition state.

A property of HH16-T2 shared by HH16 is that the fraction of ligated molecules for f_{eq}(ligation) increases with magnesium ion concentration. This presumably reflects the binding of one or more magnesium ions that are needed for ligation but not for cleavage. It is interesting that, unlike the rate data, the dependence of f_{eq}(ligation) shows simple saturating binding behavior with a relatively low $K_{app}(Mg^{2+}) = 1.6$ mM. While it is not possible to tell whether this reflects the binding of a single ion, it is striking that the value of $K_{app}(Mg^{2+})$ is much weaker for HH16 [13 mM (*29*)]. Interestingly, the value of $K_{app}(Mg^{2+})$ for the chemically cross-linked hammerhead is also tighter [6 mM (*47*)]. Thus,

it appears that the constraint imposed by the tertiary interaction and shared by the cross-link leads to tighter binding of one or more magnesium ions to the cleaved hammerhead.

The faster rate and greater extent of ligation observed for the extended hammerhead support the view that the reaction could be used to form the circular sTRSV genomes seen inside cells. Although the 50% fraction of circles seen in plant cells (*18*, *19*) for sTRSV still greatly exceeds the 6% that would form at 25 °C by our in vitro measurements, it is possible that RNA binding proteins or additional RNA elements could shift the equilibrium.

The successful dissection of k_2 and k_{-2} using the two versions of the sTRSV(+) hammerhead will make this system useful for structure−function experiments directed at understanding the mechanism of hammerhead catalysis and the role of the tertiary interactions. It is most convenient to use the HH16-T1 cleavage assay for k_2 measurements and the ligation assay with HH16-T2 to give k_{obs} and f_{eq}, thereby avoiding the difficult purification of full-length HH16-T2. Like HH16, the HH16-T1/T2 system can be considered reasonably well behaved in the sense that no kinetic heterogeneity is observed. Additionally, if HH16-T2 is assembled by combining the two products, it is fully active, making it a good candidate for structural studies.

ACKNOWLEDGMENT

We thank A. Wolfson and R. Fahlman for helpful scientific discussions.

REFERENCES

1. Symons, R. H. (1997) Plant pathogenic RNAs and RNA catalysis, *Nucleic Acids Res. 25*, 2683−2689.
2. Hutchins, C. J., Rathjen, P. D., Forster, A. C., and Symons, R. H. (1986) Self-cleavage of plus and minus RNA transcripts of avocado sunblotch viroid, *Nucleic Acids Res. 14*, 3627−3640.
3. Prody, G. A., Bakos, J. T., Buzayan, J. M., Schneider, I. R., and Bruening, G. (1986) Autolytic processing of dimeric plant-virus satellite RNA, *Science 231*, 1577−1580.
4. Prody, C. A., Zevin-Sonkin, D., Gnatt, A., Goldberg, O., and Soreq, H. (1987) Isolation and characterization of full-length cDNA clones coding for cholinesterase from fetal human tissues, *Proc. Natl. Acad. Sci. U.S.A. 84*, 3555−3559.
5. Forster, A. C., and Symons, R. H. (1987) Self-cleavage of virusoid RNA is performed by the proposed 55-nucleotide active site, *Cell 50*, 9−16.
6. Forster, A. C., and Symons, R. H. (1987) Self-cleavage of plus and minus RNAs of a virusoid and a structural model for the active sites, *Cell 49*, 211−220.
7. Uhlenbeck, O. C. (1987) A small catalytic oligoribonucleotide, *Nature 328*, 596−600.
8. Khvorova, A., Lescoute, A., Westhof, E., Jayasena, S. D., and Amgen, I. O. (2003) Sequence elements outside the hammerhead ribozyme catalytic core enable intracellular activity, *Nat. Struct. Biol. 10*, 708−712.
9. De la Peäna, M., Gago, S., and Flores, R. (2003) Peripheral regions of natural hammerhead ribozymes greatly increase their self-cleavage activity, *EMBO J. 22*, 5561−5570.
10. Garrett, T. A., Pabâon-Peäna, L. M., Gokaldas, N., and Epstein, L. M. (1996) Novel requirements in peripheral structures of the extended satellite 2 hammerhead, *RNA (New York) 2*, 699−706.
11. Pley, H. W., Flaherty, K. M., and McKay, D. B. (1994) Three-dimensional structure of a hammerhead ribozyme, *Nature 372*, 68−74.
12. Scott, W. G., Finch, J. T., and Klug, A. (1995) The crystal structure of an all-RNA hammerhead ribozyme: a proposed mechanism for RNA catalytic cleavage, *Cell 81*, 991−1002.
13. Osborne, E. M., Schaak, J. E., and Derose, V. J. (2005) Characterization of a native hammerhead ribozyme derived from schistosomes, *RNA (New York) 11*, 187−196.
14. Canny, M. D., Jucker, F. M., Kellogg, E., Khvorova, A., Jayasena, S. D., and Pardi, A. (2004) Fast cleavage kinetics of a natural hammerhead ribozyme, *J. Am. Chem. Soc. 126*, 10848−10849.
15. Penedo, J. C., Wilson, T. J., Jayasena, S. D., Khvorova, A., and Lilley, D. M. (2004) Folding of the natural hammerhead ribozyme is enhanced by interaction of auxiliary elements, *RNA (New York) 10*, 880−888.
16. Buzayan, J. M., Hampel, A., and Bruening, G. (1986) Nucleotide sequence and newly formed phosphodiester bond of spontaneously ligated satellite tobacco ringspot virus RNA, *Nucleic Acids Res. 14*, 9729−9743.
17. Bussiáere, F., Lehoux, J., Thompson, D. A., Skrzeczkowski, L. J., and Perreault, J. (1999) Subcellular localization and rolling circle replication of peach latent mosaic viroid: hallmarks of group A viroids, *J. Virol. 73*, 6353−6360.
18. Buzayan, J. M., van Tol, H., Zalloua, P. A., and Bruening, G. (1995) Increase of satellite tobacco ringspot virus RNA initiated by inoculating circular RNA, *Virology 208*, 832−837.
19. Passmore, B. K., and Bruening, G. (1993) Similar structure and reactivity of satellite tobacco ringspot virus RNA obtained from infected tissue and by in vitro transcription, *Virology 197*, 108−115.
20. Hertel, K. J., Herschlag, D., and Uhlenbeck, O. C., (1994) A kinetic and thermodynamic framework for the hammerhead ribozyme reaction, *Biochemistry 33*, 3374−3385.
21. Milligan, J. F., and Uhlenbeck, O. C. (1989) Synthesis of small RNAs using T7 RNA polymerase, *Methods Enzymol. 180*.
22. Wincott, F., DiRenzo, A., Shaffer, C., Grimm, S., Tracz, D., Workman, C., Sweedler, D., Gonzalez, C., Scaringe, S., and Usman, N. (1995) Synthesis, deprotection, analysis and purification of RNA and ribozymes, *Nucleic Acids Res. 23*, 2677−2684.
23. Hertel, K. J., Herschlag, D., and Uhlenbeck, O. C. (1996) Specificity of hammerhead ribozyme cleavage, *EMBO J. 15*, 3751−3757.
24. Feig, A. L., Ammons, G. E., and Uhlenbeck, O. C. (1998) Cryoenzymology of the hammerhead ribozyme, *RNA (New York) 4*, 1251−1258.
25. Stage-Zimmermann, T. K., and Uhlenbeck, O. C. (1998) Hammerhead ribozyme kinetics, *RNA (New York) 4*, 875−889.
26. Curtis, E. A., and Bartel, D. P. (2001) The hammerhead cleavage reaction in monovalent cations, *RNA (New York) 7*, 546−552.
27. O'Rear, J. L., Wang, S., Feig, A. L., Beigelman, L., Uhlenbeck, O. C., and Herschlag, D. (2001) Comparison of the hammerhead cleavage reactions stimulated by monovalent and divalent cations, *RNA (New York) 7*, 537−545.
28. Long, D. M., and Uhlenbeck, O. C. (1994) Kinetic characterization of intramolecular and intermolecular hammerhead RNAs with stem II deletions, *Proc. Natl. Acad. Sci. U.S.A. 91*, 6977−6981.
29. Hertel, K. J., and Uhlenbeck, O. C., (1995) The internal equilibrium of the hammerhead ribozyme reaction, *Biochemistry 34*, 1744−1749.
30. Clouet-d'Orval, B., Stage, T. K., and Uhlenbeck, O. C. (1995) Neomycin inhibition of the hammerhead ribozyme involves ionic interactions, *Biochemistry 34*, 11186−11190.
31. Fedor, M. J., and Uhlenbeck, O. C. (1990) Substrate sequence effects on "hammerhead" RNA catalytic efficiency, *Proc. Natl. Acad. Sci. U.S.A. 87*, 1668−1672.
32. Fedor, M. J., and Uhlenbeck, O. C. (1992) Kinetics of intermolecular cleavage by hammerhead ribozymes, *Biochemistry 31*, 12042−12054.
33. Dahm, S. C., Derrick, W. B., and Uhlenbeck, O. C. (1993) Evidence for the role of solvated metal hydroxide in the hammerhead cleavage mechanism, *Biochemistry 32*, 13040−13045.
34. Rojas, A. A., Vazquez-Tello, A., Ferbeyre, G., Venanzetti, F., Bachmann, L., Paquin, B., Sbordoni, V., and Cedergren, R. (2000) Hammerhead-mediated processing of satellite pDo500 family transcripts from *Dolichopoda* cave crickets, *Nucleic Acids Res. 28*, 4037−4043.
35. Ruffner, D. E., Stormo, G. D., and Uhlenbeck, O. C. (1990) Sequence requirements of the hammerhead RNA self-cleavage reaction, *Biochemistry 29*, 10695−10702.
36. Dahm, S. C., and Uhlenbeck, O. C. (1991) Role of divalent metal ions in the hammerhead RNA cleavage reaction, *Biochemistry 30*, 9464−9469.

37. Inoue, A., Takagi, Y., and Taira, K. (2004) Importance in catalysis of a magnesium ion with very low affinity for a hammerhead ribozyme, *Nucleic Acids Res. 32*.
38. Perreault, J. P., Labuda, D., Usman, N., Yang, J. H., and Cedergren, R. (1991) Relationship between 2′-hydroxyls and magnesium binding in the hammerhead RNA domain—a model for ribozyme catalysis, *Biochemistry 30*, 4020−4025.
39. Yang, J. H., Usman, N., Chartrand, P., and Cedergren, R. (1992) Minimum ribonucleotide requirement for catalysis by the RNA hammerhead domain, *Biochemistry 31*, 5005−5009.
40. Hampel, K. J., and Burke, J. M. (2003) Solvent protection of the hammerhead ribozyme in the ground state: Evidence for a cation-assisted conformational change leading to catalysis, *Biochemistry 42*, 4421−4429.
41. Rueda, D., Wick, K., McDowell, S. E., and Walter, N. G. (2003) Diffusely bound Mg^{2+} ions slightly reorient stems I and II of the hammerhead ribozyme to increase the probability of formation of the catalytic core, *Biochemistry 42*, 9924−9936.
42. Murray, J. B., Seyhan, A. A., Walter, N. G., Burke, J. M., and Scott, W. G. (1998) The hammerhead, hairpin and VS ribozymes are catalytically proficient in monovalent cations alone, *Chem. Biol. 5*, 587−595.
43. Long, D. M., LaRiviere, F. J., and Uhlenbeck, O. C. (1995) Divalent metal ions and the internal equilibrium of the hammerhead ribozyme, *Biochemistry 34*, 14435−14440.
44. Hertel, K. J., Stage-Zimmermann, T. K., Ammons, G., and Uhlenbeck, O. C. (1998) Thermodynamic dissection of the substrate-ribozyme interaction in the hammerhead ribozyme, *Biochemistry 37*, 16983−16988.
45. Weinberg, M. S., and Rossi, J. J. (2005) Comparative single-turnover kinetic analyses of trans-cleaving hammerhead ribozymes with naturally derived non-conserved sequence motifs, *FEBS Lett. 579*, 1619−1624.
46. Wang, S., Karbstein, K., Peracchi, A., Beigelman, L., and Herschlag, D. (1999) Identification of the hammerhead ribozyme metal ion binding site responsible for rescue of the deleterious effect of a cleavage site phosphorothioate, *Biochemistry 38*, 14363−14378.
47. Stage-Zimmermann, T. K., and Uhlenbeck, O. C. (2001) A covalent crosslink converts the hammerhead ribozyme from a ribonuclease to an RNA ligase, *Nat. Struct. Biol. 8*, 863−867.
48. Blount, K. F., and Uhlenbeck, O. C. (2002) Internal equilibrium of the hammerhead ribozyme is altered by the length of certain covalent cross-links, *Biochemistry 41*, 6834−6841.
49. Persson, T., Hartmann, R. K., and Eckstein, F. (2002) Selection of hammerhead ribozyme variants with low Mg^{2+} requirement: Importance of stem-loop II, *ChemBioChem 3*, 1066−1071.
50. Hertel, K. J., Pardi, A., Uhlenbeck, O. C., Koizumi, M., Ohtsuka, E., Uesugi, S., Cedergren, R., Eckstein, F., Gerlach, W. L., Hodgson, R., et al. (1992) Numbering system for the hammerhead, *Nucleic Acids Res. 20*, 3252.

BI051130T